Materials Science Forum Vols. 660-661 (2010) pp 379-384
Online available since 2010/Oct/25 at www.scientific.net

doi:10.4028/www.scientific.net/MSF.660-661.379

Effect of Cr_3C_2-NiCr Powder Characteristics on Structure and Properties of Thermal Sprayed Nanostructured Coatings.

Padial, A (1); Cunha, C.A. (1); Correa, O.V.(1); N.B. de Lima (1); Ramanathan, L.V.(1)
Instituto de Pesquisas Energéticas e Nucleares IPEN-CNEN-SP
Av. Prof. Lineu Prestes 2242, Cidade Universitaria
São Paulo.

1. INTRODUCTION

In most engineering fields there is increasing demand for materials with enhanced physical properties. Components of complex systems exposed to severe environments often require coatings for adequate thermal insulation and to prevent wear, erosion and/or oxidation. Coatings prepared with nanostructured material have, in general, exhibited higher hardness and strength compared to conventional coatings. This paper presents the microstructure, mechanical properties, thermal stability and erosion-oxidation resistance of HVOF (High Velocity Oxygen Fuel) sprayed coatings of Cr_3C_2-X(Ni20Cr) prepared using nanocrystalline and as-received (AR) powder as feedstock. Details about nanocrystalline powder synthesis and characterization are also presented.

2. MATERIALS AND METHODS

Cr_3C_2-X(Ni20Cr) powders were milled in a high energy mill (ZOZ). The powder milling parameters were: 400 rpm, ball to powder ratio 10:1 and milling times of 2, 4, 8, 16, 24 h. The milling was carried out in two different media: gaseous nitrogen and liquid hexane. Powder particle and crystallite sizes were determined using a particle size analyzer and by x-ray diffraction analysis, respectively. The mean crystallite size as a function of milling time and media was determined using the Scherrer equation, the details of which can be found elsewhere [1, 2, 5].

AISI 310 stainless steel samples (50x20x2mm) were HVOF thermal spray coated using Cr_3C_2-X(Ni20Cr) powders (X= 0, 20 and 25 wt%) in the "as received" (AR) and "nanostructured" (NS) (high energy milled) condition. The mean particle size of the powders used was about 20μm. The coating thickness varied from 50-200 μm. A scanning electron microscope coupled to an energy dispersive spectrometer was used to examine the morphology/microstructure and to determine the composition of the different phases. The chemical composition of the powders was determined by x-ray fluorescence analysis. The Vickers hardness of the coatings was also determined with loads of 300, 500 and 1000g, depending on the coating thickness. The fracture toughness of the coatings was determined qualitatively, based on the length of the cracks emanating from the hardness indents.

The erosion-oxidation (E-O) experiments were performed in a specific apparatus. In this apparatus the erosion-oxidation conditions were simulated by rotating the specimens through a fluidized bed of erodent particles. In this study the following E-O conditions were used: 200μm alumina particles as the erodent, impact velocity of 15 m/s, temperature of 500ºC and test duration of 5 hours.

The effect of heat treating (700 – 1000ºC for 2 hours, followed by air cooling) on Cr_3C_2-X(Ni20Cr) coating hardness was also determined.

3. RESULTS AND DISCUSSION

3.1. Mean particle and crystallite size.

The mean particle size of Cr_3C_2-25(Ni20Cr) powders decreased with milling time in both media, as has been reported in the literature [3, 4]. The mean particle size reduction in gaseous nitrogen was significantly more than that in liquid hexane.

The XRD spectra of the milled powders were used to determine the crystallite size. The diffraction peaks of the milled Cr_3C_2-25(Ni20Cr) powders were identified and the Cr_3C_2 reflection for $2\theta \sim 39^o$ was used to determine de crystallite size, utilizing Scherrer's equation. Taking into consideration that microstrain and equipment conditions also influence diffraction pick broadening, Gaussian fitting, related to microstrain, and Lorentzian fitting, attributed to crystallite size, were done for the selected diffraction peak in the spectra. These fittings indicated that peak broadening was due mainly to crystallite size. Fig. 1 shows the variation in mean crystallite size of Cr_3C_2-25(Ni20Cr) powder as a function of milling time. The mean crystallite size of Cr_3C_2-25(Ni20Cr), after 16 hours of milling in gaseous nitrogen reduced to 65 nm, whereas it reduced to only 105 nm in liquid hexane. The effect of hexane on the mean crystallite and particle size of Cr_3C_2-25(Ni20Cr) powder has been reported elsewhere [5].

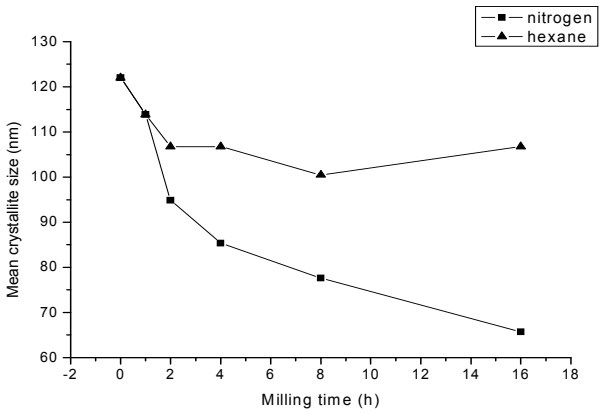

Fig.1: Variation of mean crystallite size of Cr_3C_2-25(Ni20Cr) powder as a function of milling time and the atmosphere utilized (nitrogen or hexane).

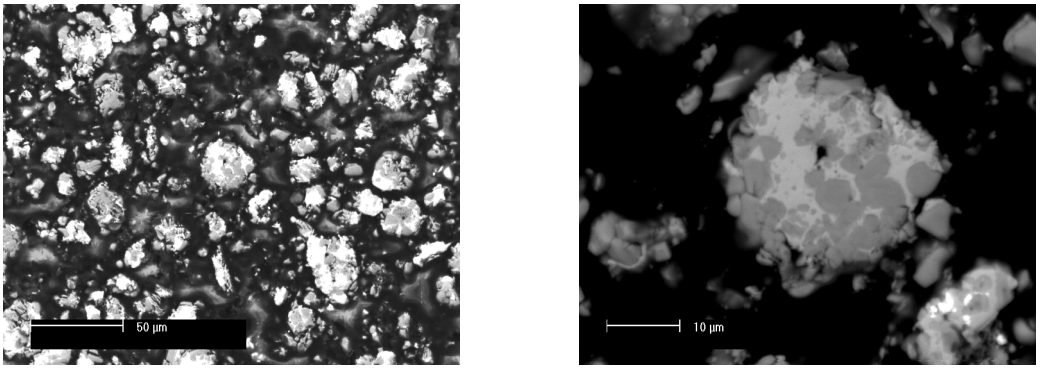

(a) (b)

Fig. 2: Secondary electrons image of the milled Cr_3C_2-25(Ni20Cr) powder (4 hour in nitrogen).

3.2 Powder particles morphology.

The Cr_3C_2-25(Ni20Cr) powder in the AR condition was homogeneous and spherical whereas the milled powder was irregular with faceted particles. Fig. 2 shows the micrographs of the powder milled for 4 hours in nitrogen. EDS analyses of dark regions revealed 95 wt% Cr, indicating it to be mainly Cr_3C_2, and the white regions (with 73 wt% Ni and 27 wt% Cr), the metallic phase Ni-Cr (binder).

3.3. Coating characteristics

3.3.1. Morphology and composition.
The micrographs in Fig. 3 show the coating surfaces prepared with AR and NS Cr_3C_2-25(Ni20Cr) powders. No significant morphological differences could be observed.

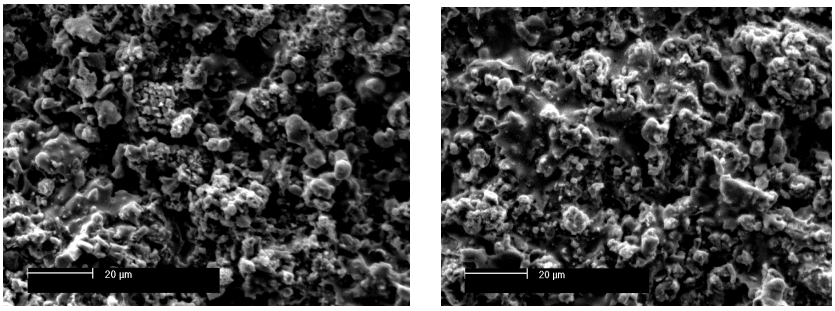

(a) (b)

Fig. 3: Micrographs of coating surfaces prepared with Cr_3C_2-25(Ni20Cr) powders: (a) AR, (b) NS.

AISI 310 samples coated with the other powders of the Cr_3C_2-X(Ni20Cr) system revealed some differences in surface morphologies. Comparison of Cr_3C_2 coatings with Cr_3C_2-(Ni20Cr) coatings, independent of the condition of the powders (AR or NS), revealed some flattened regions in the latter, due to melting of the metallic phase. The micrographs in Fig. 4 reveal cross sections of coatings prepared with Cr_3C_2-25(Ni20Cr) powders. The NS coating is less porous, more uniform and dense (Fig. 4b) compared to coatings prepared with AR powders (Fig. 4a). EDS analysis revealed large Ni peaks and very small Cr peaks on the white regions, indicating that these were mainly the metallic phase Ni-Cr. The dark regions showed large Cr peaks, suggesting these to be the Cr_3C_2 phase. The light grey regions presented both phases, Cr_3C_2 and Ni-Cr, indicating a composite phase [6].

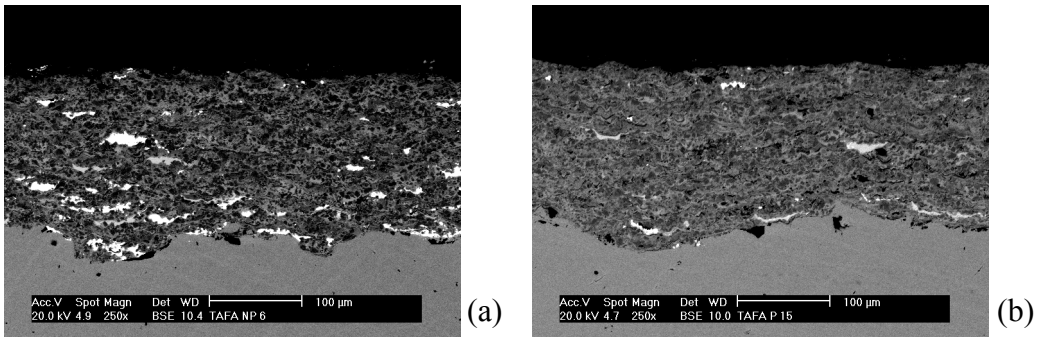

(a) (b)

Fig. 4: Micrographs of Cr_3C_2-25(Ni20Cr) coating cross sections: (a) AR and (b) NS.

3.3.2. Hardness

Tab. 1 shows the Vickers microhardness of Cr_3C_2-25(Ni20Cr) coatings. Vickers microhardness of NS coatings is higher than that of the coatings produced AR powders. The table also shows that hardness increased with increase in coating thickness. This could be attributed to thermal effects produced in the top layer due to heat dissipation from the previous layer. Further proof of this was observed when the effect of heat treatment on coating hardness was studied.

Tab. 1: Vickers microhardness of coatings produced with Cr_3C_2-25(Ni20Cr) powders in the AR and NS condition.

	Vickers hardness of Cr_3C_2-25(Ni20Cr) (GPa)					
	AR			NS		
Coating thickness (µm)	56	190	234	73	175	214
Load-500 g	6,66	7,94	9,40	9,58	10,06	11,03
Load-1000 g	4,17	7,80	6,56	8,12	6,83	10,42

Cracks emanating from the indents were observed on both types of coatings (Fig. 5). Cracks in the coating produced with AR powders were longer and wider. Most of the cracks propagated in the direction parallel to the substrate. Similar observations have been reported in the literature [3, 7]. The crack length was used qualitatively to compare fracture toughness of the coatings. Comparison of the cracks in both types of coatings revealed that NS coatings had higher fracture toughness. Some cracks were also observed at interface boundaries, probably due to the formation of composites with higher hardness.

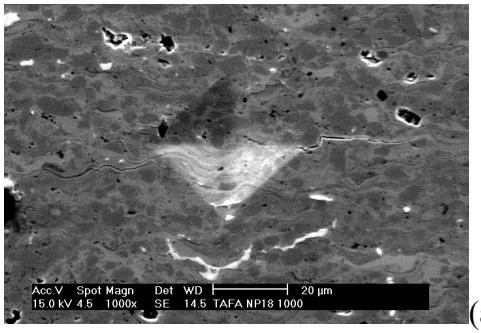

(a)

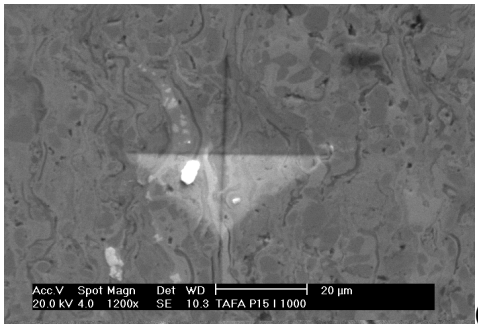

(b)

Fig. 5: Vickers hardness indents on Cr_3C_2-25(Ni20Cr) coating cross sections: (a) AR and (b) NS.

Tab. 2: Vickers hardness and elastic modulus for NS coatings produced with different powders.

Powders Composition	Vickers Hardness (GPa)	Young Modulus (GPa)
Cr_3C_2	14,33	267,05
Cr_3C_2-20Ni20Cr	10,95	282,37
Cr_3C_2-25Ni20Cr	10,12	245,75

Tab. 2 presents the Vickers hardness and elastic modulus of NS coatings produced with Cr_3C_2-X(Ni20Cr). The hardness decreased with increasing metallic phase (Ni-Cr) content. On the other hand, no trends were observed regarding the elastic modulus. It is important to note that the hardness of coatings prepared by the HVOF method is influenced by the deposition technique and by feedstock powder characteristics [8]. In the HVOF process the particle velocity is high and thermal energy is low, factors that usually result in higher hardness. Despite the fact that majority of the data in the literature indicate that NS materials have higher hardness than corresponding

conventional materials, there are several studies pointing out that this hardness increase is not as high as that predicted by the classical Hall-Petch equation [9].

3.3.3. Erosion-oxidation behavior

Erosion-oxidation (E-O) experiments were performed with only the Cr_3C_2-25(Ni20Cr) coatings. Wastage of the coated specimens was determined after 5 hours at 500ºC. The surface roughness of the samples was measured before and after the experiments. The results of these studies, shown in Tab. 3, indicate a significant increase in E-O resistance of the samples coated with NS powders. The surface roughness of the samples decreased regardless of the condition of the powder (AR or nanocrystalline) used to prepare the coating.

Tab. 3: Erosion-oxidation results for samples coated with Cr_3C_2-25(Ni20Cr) powders.

Coating		Wear 10^{-3} g cm^{-2}	Surface Roughness (Ra) (μm)	
Type	Condition		Initial	Final
Cr_3C_2-25Ni20Cr	AR	9,20	6,58	3,95
Cr_3C_2-25Ni20Cr	NS	6,00	4,38	3,36

3.3.4. Influence of heat treatment on mechanical properties

Coatings of the Cr_3C_2-X(Ni20Cr) system, in both conditions (AR and NS) were heat treated at 700ºC, 800ºC, 900ºC and 1000ºC for 2 hours and air cooled. After these heat treatments microhardness measurements were performed on cross sections of the samples. Fig. 6 shows the variation in hardness of the Cr_3C_2-20(Ni20Cr) coatings as a function of temperature.

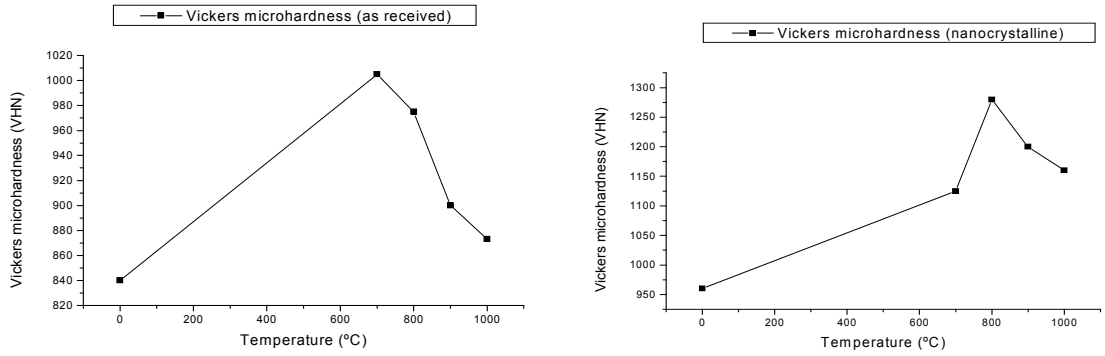

(a) (b)

Fig. 6: Vickers microhardness variation of Cr_3C_2-20(Ni20Cr) coating as a function of heat treatment temperature: (a) AR; (b) NS.

The hardness of all the coatings treated at 700ºC was always higher than that prior to heat treatment. As a general rule, as the temperature increased, the hardness of all the coatings increased up to a maximum and then decreased. This maximum hardness value and the temperature at which it happened varied with the type of coating. In the case of the Cr_3C_2 coating, the hardness was much higher than that of the coating with the metallic phase Ni-Cr. The temperature at which the maximum hardness was obtained for the Cr_3C_2 coating was higher for that prepared with AR powder. In the case of the Cr_3C_2 with a metallic phase Ni20Cr, the maximum Vickers hardness for the coating in the AR condition (1000 kgf/mm^2) was achieved at 700ºC, while for the same coating but NS, the maximum (1250 kgf/mm^2) was obtained at 800ºC. This indicates that the maximum hardness value for NS coatings is not only higher, but is achieved at higher temperatures,

suggesting improved microstructure stability of the NS coating. Similar observations were made with the coating with 25wt % of the metallic phase, i.e., Cr_3C_2-25(Ni20Cr) powder.

The hardness indents were examined and several cracks were observed. All the indents on the AR and NS Cr_3C_2 coatings revealed cracks independent of the heat treatment temperature, indicating the brittle nature and the low fracture toughness of this coating. On the other hand, in the Cr_3C_2-20(Ni20Cr) coatings prepared with AR powder, the indents revealed cracks only at hardness values higher than 850 kgf/mm^2, while coatings produced with nanocrystalline powder revealed cracks only at hardness values above 1000 kgf/mm^2. Similarly, the coatings produced with NS Cr_3C_2-25(Ni20Cr) powder revealed cracks only at hardness values higher than 1200 kgf/mm^2. These observations indicate that the NS coatings have higher resistance to crack formation, compared to coatings prepared with AR powders. The increase in metallic phase content in NS coatings prepared from Cr_3C_2-X(Ni20Cr) increased the fracture toughness.

4. CONCLUSIONS

1. A significant reduction in the mean particle and crystallite size with increase in milling time was observed.
2. The microstructure of NS Cr_3C_2-25(Ni20Cr) coatings was more uniform compared to coatings prepared with AR powders.
3. The hardness, fracture toughness, erosion-oxidation resistance and thermal stability in the range 700 – 1000ºC, of NS Cr_3C_2-25(Ni20Cr) coatings was higher than that of coatings prepared with AR powders.

References

1. Klug HP, Alexander LE. X-ray Diffraction Procedures, Wiley, New York. 1974; 643.
2. Keijser ThHde, Langford JI, Mittemeijer EJ, Vogels ABP. Use of the Voight function in a single-line method for the analysis of x-diffraction line broadening. *Journal of Applied Crystallography*. 1982; 15: 308-314.
3. He J, Ice M, Lavernia EJ. Synthesis and characterization of nanostructured Cr_3C_2-NiCr. *Nanostructured Materials*. 1998; 10: 1271-1283.
4. He J, Schoenung JM. Nanostructured coatings, *Materials Science and Engineering*. 2002; A336: 274-319.
5. Cunha CA, Padial AGF, Lima NB, Martinelli JR, Correa OV, Ramanathan LV. Effect of high energy milling parameters on nanostructured Cr_3C_2-Ni20Cr powder characteristics, Materials Science Forum – Vols. 591-593 (2008) pp 282-288.
6. Roy M, Pauschitz A, Bernardi J, Koch T, Franek F. Microstructure and mechanical properties of HVOF sprayed nanocrystalline Cr_3C_2-25(Ni20Cr) coatings. *Journal of Thermal Spray Technology*. 2006; 15(3): 372-381.
7. Russo L, Dorfmann M. High temperature oxidation of MCrAlY coatings produced by HVOF in Thermal Spraying: Current status and future trends, A.Ohmori Ed.. High Temperature Society of Japan, Osaka, Japan, 1995, 681-686.
8. Vuoristo P, Niemi T, Mantyla T, Berger LM, Nebelung M. Comparison of different hardmetal-like coatings sprayed by plasma and detonation gun processes, Proceedings of 8th National Thermal Spray Conference 1995, CC Brendt and S Sampath, Eds., Houston, USA, ASM International: Materials Park, OH, USA. 1995; 309.
9. Usmani S, Sampath S, Herman H. Thermal stability of nanocrystalline WC-Co powder synthesized by using mechanical milling at low temperature, in Thermal Spray Processing of Nanoscale Materials - A Conference Report with Extended Abstracts, CC Brendt and EJ Lavernia eds: *Journal of Thermal Spray Technology*. 1998; 7: 429-431.

Advanced Powder Technology VII
doi:10.4028/www.scientific.net/MSF.660-661

Effect of Cr₃C₂-NiCr Powder Characteristics on Structure and Properties of Thermal Sprayed Nanostructured Coatings
doi:10.4028/www.scientific.net/MSF.660-661.379